ISSN:2320-0790

An International Journal of Advanced Computer Technology

# An Enhanced Level Set Segmentation for Multichannel Images Using Fuzzy Clustering and Lattice Boltzmann Method

[1]Savita Agrawal, [2]Deepak Kumar Xaxa
[1]PG Student, Dept of Computer science, Mats University Raipur, India
[2]Assistant Professor, Dept. of computer science, Mats University Raipur, India

**Abstract**— In the last decades, image segmentation has proved its applicability in various areas like satellite image processing, medical image processing and many more. In the present scenario the researchers tries to develop hybrid image segmentation techniques to generates efficient segmentation. Due to the development of the parallel programming, the lattice Boltzmann method (LBM) has attracted much attention as a fast alternative approach for solving partial differential equations. In this project work, first designed an energy functional based on the fuzzy c-means objective function which incorporates the bias field that accounts for the intensity in homogeneity of the real-world image. Using the gradient descent method, corresponding level set equations are obtained from which we deduce a fuzzy external force for the LBM solver based on the model by Zhao. The method is speedy, robust for denoise, and does not dependent on the position of the initial contour, effective in the presence of intensity in homogeneity, highly parallelizable and can detect objects with or without edges. For the implementation of segmentation techniques defined for gray images, most of the time researchers determines single channel segments of the images and superimposes the single channel segment information on color images. This idea leads to provide color image segmentation using single channel segments of multi channel images. Though this method is widely adopted but doesn't provide complete true segmentation of multichannel ie color images because a color image contains three different channels for Red, green and blue components. Hence segmenting a color image, by having only single channel segments information, will definitely loose important segment regions of color images. To overcome this problem this paper work starts with the development of Enhanced Level Set Segmentation for single channel Images Using Fuzzy Clustering and Lattice Boltzmann Method. For the implementation of the proposed method over color images the input color image will be first divided into red, green and blue single channels then by applying the proposed single channel technique on each channels of color image will lead to three different segmentation information for red, green and blue channels. After combining all the three segmentation information true color image segments will be obtained.

For the comparative analysis of the proposed segmentation scheme three segmentation parameters have been utilized, they are Probabilistic Rand Index (PRI), Variation of Information (VOI) and Global Consistency Error (GCE). A huge comparative analysis is performed for comparison on the basis of these three parameters. The results obtained clearly indicates that the proposed technique for color image segmentation is efficient as compare to existing technique in all the aspects of segmentation.

**Key words:** Fuzzy c-means (FCM), image segmentation, intensity in-homogeneity, lattice Boltzmann method (LBM), level set equation (LSE), partial differential equation (PDE).

## I. INTRODUCTION

In computer vision, image segmentation [38]–[40] is a major and nontrivial task which aims to partition a given image into several regions or to detect an object of interest from the background. This task is more challenging that most of the actual imaging devices produce images corrupted by intensity in-homogeneity. The level set method (LSM) is a part of the whole family of active contour methods (ACMs). The key idea that started the level set fanfare was the Hamilton–Jacobi approach, i.e., a time-dependent equation for a moving surface. This was first done in the seminal work of Osher and Sethian [1]. In 2-D space, the LSM represents a closed curve in the plane as the zero level set of a 3-D function Ø. For instance, starting with a curve around the object to be detected, the curve travels toward its inner normal and has to stop on the boundary of the object. Two approaches are usually used to stop the evolving curve on the boundary of the desired object; the first one uses an edge indicator depending on the gradient of the image like in classical snakes and ACMs [2]–[5], [21], [31], and the second one uses some regional attributes to stop the evolving curve on the actual boundary [22], [23], [32] where the authors extend the representative region-based level set from scalar to tensors by simultaneously taking into account the pixel's gray level and some local statistics such as gradient and orientation. The latter is more robust against noise and can detect objects without edges.

In addition, the Chan Vese (CV) method is not suitable for parallel programming because, at each iteration, the average intensities inside and outside the contour should be computed, which increases drastically the CPU time by increasing communications between processors. For this purpose, we propose a new method which tries to overcome the aforementioned drawbacks. Our method is based on a new idea which aims to stop the evolving curve according to the membership degree of the current pixel to be inside or outside of the active contour. This is done with the help of the modified fuzzy C-means (FCM) objective function obtained in [19] which also takes into consideration the shading image due to the intensity in-homogeneity.

In the LSM, the movement of the zero level set is actually driven by the level set equation (LSE), which is a partial differential equation (PDE). For solving the LSE, most classical methods such as the upwind scheme are based on some finite difference, finite volume or finite element approximations and an explicit computation of the curvature [20].Unfortunately, these methods cost a lot of CPU time.

Recently, the lattice Boltzmann method (LBM) has been used as an alternative approach for solving LSE [12], [14], [29], [36]. It can better handle the problem of time consuming because the curvature is implicitly computed and the algorithm is simple and highly parallelizable.

In this paper, the LBM is used to solve the LSE. The proposed method is based on the approach of the LBM PDE solver defind in [14]. In our proposed method, using a modified FCM objective function, we design a new fuzzy external force (FEF). The method is fast, robust against noise, and efficient whatever the position or the shape of the initial contour and can detect efficiently objects with or without edges. It has, first, the advantage of the FCM which gives it the latitude to stop the evolving curve according to the membership degree of the current pixel, second, the advantages of the LSM which allow it to handle complex shapes, topological changes, and different constraints on the contour smoothness, speed, size, and shape which are easily specified, and, third, the advantages of the LBM which make it very suitable for parallel programming due to its local and explicit nature.

## II. BACKGROUND

The proposed method uses mainly two techniques belonging to different frameworks: the LSM and the LBM.

### *A. LSM*

The LSM is a numerical technique for tracking interfaces and shapes. Using an implicit representation of active contours, it has the advantage of handling automatically topological changes of the tracked shape. In 2-D image segmentation, the LSM represents a closed curve as the zero level set of $\varphi$, called the level set function. The evolution of the curve starts from an arbitrary starting contour and evolves itself driven by the LSE which can be seen as a convection–diffusion equation

$$\frac{\partial \theta}{\partial t} + \vec{V} \cdot \nabla \phi = b \Delta \phi \quad \ldots (1)$$

Where $\nabla\emptyset$ and $\Delta\emptyset$ are the gradient and the Laplacian of $\emptyset$, respectively. The term $b\Delta\emptyset$ is called artificial viscosity (Sethian suggested replacing it with $bk|\nabla\emptyset|$ which is better for handling the evolution of lower dimensional interfaces [12]), and $k$ is the curvature of the distance function $\emptyset$. The LSE can therefore be written as

$$\frac{\partial \theta}{\partial t} + \vec{V} \cdot \nabla \phi = bk|\Delta \phi|. \quad \ldots (2)$$

Being an alternative method for solving PDE, the LBM has several advantages, such as parallelizability and simplicity. In this paper, we use the D2Q9 LBM model to resolve the LSE in 2-D space.

### *B. LBM*

The LBM is a numerical framework for modeling Boltzmann particle dynamics on a 2-D or 3-D lattice [13]. It was first designed to solve macroscopic fluid dynamics problems [14]. The method is second order accurate both in time and in Fig. 1. Spatial structure of the D2Q9 LBM lattice. space, and in the limit of zero time step and lattice spacing, it yields the Navier Stokes equations for an incompressible fluid [15].

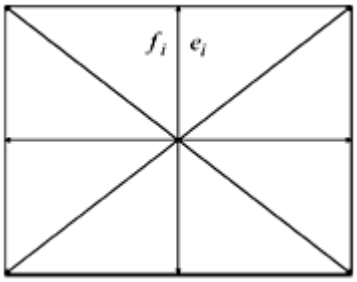


Fig. (1) Spatial structure of the D2Q9 LBM lattice.

The proposed method uses the D2Q9 (2-D with eight links with its neighbors and one link for the cell itself) LBM lattice structure. Fig. 1 shows a typical D2Q9 model. Each link has its velocity vector $e_i(\vec{r}, t)$ and the particle distribution $f_i(\vec{r}, t)$ that moves along this link, where $\vec{r}$ is the position of the cell, and $t$ is the time. The LBM evolution equation can be written as follows using the Bhatnagar, Gross, and Krook collision model [7].

$$f_i(\vec{r} + \vec{e}_i, t+1) = f_i(\vec{r}, t) + \frac{1}{\tau}\left[f_i^{eq}(\vec{r}, t) - f_i(\vec{r}, t)\right] \quad \ldots(3)$$

where $\tau$ represents the relaxation time determining the kinematic viscosity $\vartheta$ of the fluid by

$$\vartheta = \frac{1}{3}\left(\tau - \frac{1}{2}\right) \quad \ldots(4)$$

and *f*eq *i* is the equilibrium particle distribution defined as

$$f_i^{eq}(\rho, \vec{u}) = \rho\left(A_i + B_i(\vec{e}_i \cdot \vec{u}) + C_i(\vec{e}_i \cdot \vec{u})^2 + D_i(\vec{u})^2\right) \quad \ldots(5)$$

Where *Ai* to *Di* are constant coefficients depending on the geometry of the lattice links and $\rho$ and $\vec{u}$ are the macroscopic fluid density and velocity, respectively, computed from the particle distributions as

$$\rho = \sum_i f_i \quad \vec{u} = \frac{1}{\rho}\sum_i f_i \vec{e}_i. \qquad \ldots (6)$$

For modeling typical diffusion computations, the equilibrium function can be simplified as follows [14]: *f*eq

$$f_i^{eq}(\rho, \vec{u}) = \rho A_i. \qquad \ldots (7)$$

In the case of D2Q9 model, *Ai* = 4/9 for the zero link, *Ai* = 1/9 for the axial links, and *Ai* = 1/36 for the diagonal links. Now, the relaxation time $\tau$ is determined by the diffusion coefficient $\gamma$ defined as

$$\gamma = \frac{2}{9}(2\tau - 1) \qquad \ldots (8)$$

As shown in [14], LBM can be used to solve the parabolic diffusion equation which can be recovered by the Chapman–Enskog expansion

$$\frac{\partial \rho}{\partial t} = \gamma \nabla \cdot \nabla \rho. \qquad \ldots (9)$$

In this case, the external force can be included as follows:

$$f_i \leftarrow f_i + \frac{2\tau - 1}{2\tau} B_i(\vec{F} \cdot \vec{e}_i) \qquad \ldots (10)$$

Moreover, thus, (9) becomes

$$\frac{\partial \rho}{\partial t} = \gamma \nabla \cdot \nabla \rho + F. \qquad \ldots (11)$$

Replacing $\rho$ by the signed distance function ∅, the LSE can be formed.

## III. PROPOSED METHODOLOGY

This section details first the conception of the FCM-based energy function from which we deduce the corresponding LSE. We then set the FEF. Moreover, finally, we implement the proposed method.

### *A. Energy Function Design*

In the image segmentation context, the standard FCM algorithm is an optimization problem for partitioning an image of N pixels, X = $\{xi\}^N_{i=1}$,intoc classes. It aims to minimize a clustering criterion as [7]

$$J(U,V,X) = \sum_{k=1}^{c}\sum_{i=1}^{N} u_{ki}^p \|x_i - v_k\|^2$$

$$\text{s.t.} \sum_{k=1}^{c} u_{ki} = 1 \;\forall i \qquad 0 \le u_{ki} \le 1 \;\forall k, i \qquad \ldots(12)$$

Where U is the partition matrix whose element $u_{ki}$ is the membership of the $i^{th}$ voxel for $k^{th}$ class. V is the centroid vector whose element $v_k$ is the centroid (or prototype) of $k_{th}$ class. The parameter p, said to be fuzzy index, is defined as a weighting exponent on each fuzzy membership and calculates the amount of "fuzziness" of the resulting partition. The norm operator ||.|| shows the standard Euclidean distance. The objective function J is decreased when high membership values are assigned to the pixels whose intensities are close to the centroid of its particular class and low membership values are assigned to the pixels whose intensities are far from the centroid. As done in [7], the bias field is incorporated into the FCM framework by modeling the observed image as follows:

$$Y_i = X_i G_i \;\forall i \in \{1, 2, \ldots, N\} \qquad \ldots(13)$$

Where Yi, Xi, and Gi are the observed intensity, true intensity, and gain field at the $i^{th}$ pixel, respectively. N is the total number of pixels in the magnetic resonance image. The artifact can be modeled as an additive bias field by applying a logarithmic transformation to both sides of (13) [7], [8]

$$y_i = x_i + \beta_i \;\forall i \in \{1, 2, \ldots, N\} \qquad \ldots(14)$$

Where yi and xi are the observed and true log-transformed intensities at the $i^{th}$ voxel, respectively, and ß is the bias field at the $i^{th}$ voxel. By incorporating the bias field model into an FCM framework, we will be able to iteratively estimate both the true intensity and the bias field from the observed intensity. By substituting (14) into (12), the clustering criterion to minimize in the presence of bias field becomes a constrained optimization problem.

$$J(U,V,B,Y) = \sum_{k=1}^{c}\sum_{i=1}^{N} u_{ki}^p \|y_i - \beta_i - v_k\|^2$$

$$\text{s.t.} \sum_{k=1}^{c} u_{ki} = 1 \;\forall i \qquad 0 \le u_{ki} \le 1 \;\forall k, i \qquad \ldots(15)$$

Where $Y = \{y_i\}_{i=1}^N$ is the observed image and $B = \{B_i\}_{i=1}^N$ is the bias field image. In a continuous form, the aforementioned criterion can be written as

$$J(U,V,B,Y) = \sum_{k=1}^{c} \int_{\Omega_k} U_k^p(x,y)\, \|Y(x,y) - B(x,y) - v_k\|^2 \, dx$$

$$\text{s.t.} \sum_{k=1}^{c} U_k(x,y) = 1 \;\forall x, y \qquad 0 \le U_k(x,y) \le 1 \;\forall k, x, y. \qquad \ldots(16)$$

Consider the two-phase level set although the method can be easily extended to more than two phases. The image domain Ω is segmented into two disjoint regions Ω1 and Ω2, i.e., c =2.In this case, we can introduce a level set function as follows:

$$J(U,V,B,Y,\phi) = \int_\Omega U_1^p(x,y)\|Y(x,y) - B(x,y) - v_1\|^2 H(\phi) dxdy + \int_\Omega U_2^p(x,y)\|Y(x,y) - B(x,y) - v_2\|^2 (1 - H(\phi))\, dxdy$$

$$\text{s.t. } U_1(x,y) + U_2(x,y) = 1 \;\forall x, y \qquad 0 \le U_k(x,y) \le 1 \;\forall k, x, y \qquad \ldots(17)$$

Where Ø is a signed distant function. The aforementioned term J(U, V, B, Y, Ø) is used as the data link in our energy functional which is defined as follows:

$$E(U,V,B,Y,\phi) = J(U,V,B,Y,\phi) + \nu|C| \qquad \ldots(18)$$

where ν|C| is a regularization term with ν>0 being a fixed parameter and C being a given curve which is represented

implicitly as the zero level of Ø and |C| is the length of C and can be expressed by the following equation [9]

$$|C| = \int_{\Omega} |\nabla H(\phi)|\, dxdy. \quad \ldots(19)$$

*B. LSE*

As done in [10], to obtain the LSE, we minimize E(U, V, B, Y, Ø) with respect to f. For fixed U, V, and B, we use the gradient descent method

$$\frac{\partial \phi}{\partial t} = -\frac{\partial E}{\partial \phi} \quad \ldots(20)$$

Where ∂E/∂f is the Gateaux derivative [11] of E. We obtain the following LSE:

$$\begin{aligned} \frac{\partial \phi}{\partial t} &= \delta(\phi)\left(U_1^p(x,y)\,\|Y(x,y) - B(x,y) - v_1\|^2 \right. \\ &\quad \left. - U_2^p(x,y)\,\|Y(x,y) - B(x,y) - v_2\|^2\right) \\ &\quad + \nu\delta(\phi)\mathrm{div}\left(\frac{\nabla\phi}{|\nabla\phi|}\right) \\ &\text{s.t. } U_1(x,y) + U_2(x,y) = 1\ \forall x,y \\ &\quad 0 \le U_k(x,y) \le 1\ \forall k,x,y. \end{aligned} \quad \ldots(21)$$

However, for solving the minimization problem of E(U, V, B, Y, Ø), we should also compute the first derivatives of E(U, V, B, Y, Ø) with respect to u$ki$ , v$k$, and ß$i$ and set them equal to zero. We thus obtain three necessary conditions

$$U_k^*(x,y) = \frac{1}{\sum_{l=1}^{c}\left(\frac{\|Y(x,y)-B(x,y)-v_k\|}{\|Y(x,y)-B(x,y)-v_l\|}\right)^{\frac{2}{(p-1)}}} \quad \ldots(22)$$

$$v_k^* = \frac{\int_{\Omega} U_k^p(x,y)\,(Y(x,y) - B(x,y))\,dxdy}{\int_{\Omega} U_k^p(x,y)dxdy} \quad \ldots(23)$$

$$B^*(x,y) = Y(x,y) - \frac{\sum_{k=1}^{c} U_k^p(x,y)v_k}{\sum_{k=1}^{c} U_k^p(x,y)}. \quad \ldots(24)$$

*C. Lattice Boltzmann Solver for LSE*

By using the gradient projection method of Rosen [17], we can replace d(Ø) by |∇ Ø | in the proposed LSE, and as Ø is a distance function, we have |∇ Ø | =1[16], [20] and will stay at each step since an adaptive approach is not used and the distant field is valid in the whole domain [25]. Thus, the proposed LSE becomes

$$\begin{aligned} \frac{\partial \phi}{\partial t} &= U_1^p(x,y)\,\|Y(x,y) - B(x,y) - v_1\|^2 \\ &\quad - U_2^p(x,y)\,\|Y(x,y) - B(x,y) - v_2\|^2 + \nu\mathrm{div}(\nabla\phi) \\ &\text{s.t. } U_1(x,y) + U_2(x,y) = 1\ \forall x,y \\ &\quad 0 \le U_k(x,y) \le 1\ \forall k,x,y. \end{aligned} \quad \ldots(25)$$

Replacing ρ by the signed distance function Ø, (11) becomes

$$\frac{\partial \phi}{\partial t} = \gamma\mathrm{div}(\nabla\phi) + F. \quad \ldots(26)$$

By setting the external force

$$F = \lambda\left(U_1^p(x,y)\,\|Y(x,y) - B(x,y) - v_1\|^2 - U_2^p(x,y)\,\|Y(x,y) - B(x,y) - v_2\|^2\right) \quad \ldots(27)$$

Where λ is a positive parameter; we can see that (25) is only a variational formula of (26) and, thus, can be solved by the LBM with the above-defined FEF. The choice of parameter p is at great importance for the segmentation result. Different values for p will generate different results, as following.

i If p>2, then the exponent 2/(p - 1) in (22) decreases the membership value of the pixels that are closed to the centroid. The segmentation result will therefore be wrong since it is intuitively better that the membership value be high for those pixels who are closed to the centroid.

ii If p →∞, all the membership values tend to 1/c. This implies that the

$$\mathrm{FEF} \to \lambda\left(\left(\frac{1}{c}\right)^p \|Y(x,y) - B(x,y) - v_1\|^2 - \left(\frac{1}{c}\right)^p \|Y(x,y) - B(x,y) - v_2\|^2\right) \to 0.$$

There is, therefore, no link with the image data in the LSM process. Therefore, segmentation is impossible.

iii If p → 1, the exponent 2/(p - 1) increases the membership values of the pixels who are closed to the centroid. As p → 1, the membership tends to one for the closest pixels and tends to zero for all the other pixels. This case is equivalent to the use of the k-means objective function instead of the FCM one. The segmentation is therefore rigid, and we lose the advantage of FCM over k-means. For all these reasons, a suitable choice of the parameter p can be the value of two, which is therefore used in all our experiments.

## IV. IMPLEMENTATION

When using LBM to resolve the convection–diffusion equation, the particle density is set as Ø this is a signed distance function. Since the particle number of the cell cannot be negative, we modify the distance function as $\emptyset' = \emptyset - min(\emptyset)$. The contour is those pixels which satisfy $\emptyset' = -min(\emptyset)$. The steps of proposed multichannel image segmentation technique using RGB color space are outlined as follows.

i. Read the multichannel image for the segmentation as input image.
ii. Initialize the distance function Ø and class centroid values$v1$ and $v2$. Initialize $B$ with zeros.
iii. Divide the multichannel image into its constituent Red, Green and Blue components.
iv. Now apply the steps v to xiii for each separately on Red, Green and Blue components.
v. Compute $U_1^p(x,y)$ and $U_2^p(x,y)$ with (22).
vi. Compute $v1$ and $v2$ with (23).
vii. Compute B with (24).
viii. Compute the external force with (27).
ix. Include the external force based on (10).
x. Resolve the convection–diffusion equation with LBM with (3).
xi. Accumulate the $fi(\vec{r},t)$ values at each grid point by (6), which generates an updated distance value at each point.
xii. Find the contour.

xiii. If the segmentation is not done, increase the value of $\lambda$ and go back to step 5).

xiv. After getting contour for all the three separate channels (ie Red, Green and Blue Channels) combine the entire three contours to get contour for all three components.

xv. Display multichannel segmented image as output of the project work.

## V. EVALUATION OF THE PROPOSED METHOD

In order to objectively measure the quality of the segmentations produced; three evaluation measures are considered in this paper. The first one is the Probabilistic Rand Index (PRI, [21]). This index compares results obtained from the tested algorithm to a set of manually segmented images. Since there is not a single correct output, considering multiple results allows to enhance the comparison and to take into account the variability of human perception.

The PRI is based on a soft non uniform weighting of pixel pairs as a function of the variability in the ground-truth. The ground-truth set is defined as $\{G_1, G_2, \cdots, G_L\}$ where $L$ is the number of manually segmented images. Let $S$ be the segmentation provided by the tested algorithm, $l_i^{Gk}$ the label of pixel $\mathbf{x}_i$ in the $k$-th manually segmented image and $l_i^S$ the label of pixel $\mathbf{x}i$ in the tested segmentation. Then, PRI is defined by

$$PR(S, G_k) = \frac{2}{N(N-1)} \sum_{i,j,i<j} \left( p_{ij}^{c_{ij}} (1 - p_{ij})^{1-c_{ij}} \right)$$

Where $N$ is the number of pixels, $c_{ij}$ is a Boolean function denoting if $l_i^S$ is equal to $l_j^{Gk}$ , and $p_{ij}$ is the expected value of a Bernoulli distribution for the pixel pair. The PRI metric is in the range [0, 1], where high values indicate a large similarity between the segmented images and the ground-truth.

The second one is the Variation of Information (VOI, [15]). The VOI metric measures the sum of information loss and gain between two clustering belonging to the lattice of possible partitions. It is defined by

$$VOI(S, G_k) = H(S) + H(G_k) - 2I(S, G_k).$$

Where $H$ is the entropy $-\sum_{i=1}^{c} \frac{n_i}{n} log \frac{n_i}{n}$, $n_i$ being the number of points belonging to the i[th] cluster. The term I is the mutual information between two clustering, and it is defined by

$$I(S, G_k) = \sum_{i=1}^{c} \sum_{j=1}^{c} \frac{n_{i,j}}{n} \log \frac{n_{i,j}}{n} \frac{n_i}{n} \frac{n_j}{n}$$

Where $n_{i,j}$ is the number of points in the intersection of cluster $i$ of $S$ and $j$ of $G_k$. The VOI measure is a distance, therefore the smaller it is, the closer the segmentation obtained and the ground-truth are.

The Global Consistency Error (GCE [14]) evaluates to what extent a segmentation can be viewed as the refinement of the other. A measure of error at each pixel $\mathbf{x}_i$ is defined by

$$E(S, G_k, \mathbf{x}_i) = \frac{|R(S, \mathbf{x}_i) \backslash R(G_k, \mathbf{x}_i)|}{|R(S, \mathbf{x}_i)|}$$

Where $|.|$ is the cardinality, $\backslash$ is the set difference, and $R(S, \mathbf{x}i)$ is the set of pixels corresponding to the region in segmentation $S$ that contains the pixel $\mathbf{x}i$. The GCE measure, which forces all local refinements to be in the same direction, is then defined by

$$GCE(S, G_k) = \frac{1}{n} \min \left( \sum_{i=1}^{n} E(S, G_k, \mathbf{x}_i), \sum_{i=1}^{n} E(G_k, S, \mathbf{x}_i) \right)$$

The closer $GCE$ is to zero, the better the segmentation $S$ with respect to the ground-truth $G_k$.

Now in the remaining part of this section we will present the results obtained from the developed work. For the proper evaluation of the developed method five color images (Multichannel images) have been used for example figure (5.1) and figure (5.2) shows the first input image and its segmentation using proposed work. Table 1 contains the three parameter values obtained after segmentation using proposed method and exiting method. To check the effectiveness of the developed technique three plots for three parameters, have been also shown from figure (5.11) to figure (5.13).

Figure (5.1) First Input Image

Figure (5.2) Segmented Image

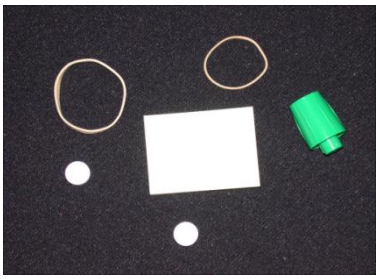

Figure (5.3) Second Input Image

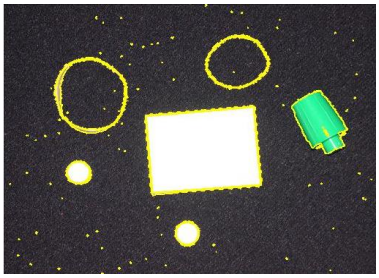

Figure (5.4) Segmented Image


Figure (5.5) Third Input Image


Figure (5.6) Segmented Image

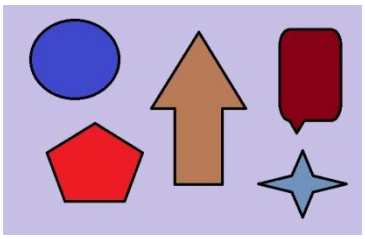

Figure (5.7) Fourth Input Image

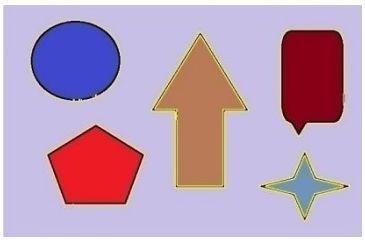

Figure (5.8) Segmented Image


Figure (5.9) Fifth Input Image


Figure (5.10) Segmented Image

Table (1)

| S. No. | PRI OLD | PRI NEW | VOI OLD | VOI NEW | GCE OLD | GCE NEW |
|---|---|---|---|---|---|---|
| 1 | 0.79065 | .772088 | 0.779141 | .818764 | 0.142078 | .145903 |
| 2 | 0.977382 | .973917 | 0.355699 | .419825 | 0.0172486 | .0194614 |
| 3 | 0.878131 | .878105 | 0.567029 | .566979 | 0.109219 | .109251 |
| 4 | 0.525675 | .527225 | 1.26532 | 1.2636 | 0.128349 | .128208 |
| 5 | 0.965934 | .965934 | 0.229382 | .229382 | 0.0330667 | .0330667 |
| 6 | 0.973822 | .973822 | 0.136113 | .136071 | 0.0158472 | 0.0158016 |
| 7 | 0.9882 | .995966 | 0.0819 | .0357325 | 0.0108 | .00394074 |
| 8 | 0.969395 | .934146 | 0.228627 | .871699 | 0.0291553 | 0.0435187 |
| 9 | 0.971685 | .970932 | 0.184803 | .189502 | 0.0262651 | .0269561 |
| 10 | 0.857307 | .889475 | 0.584679 | .521737 | 0.0929263 | 0.0847614 |

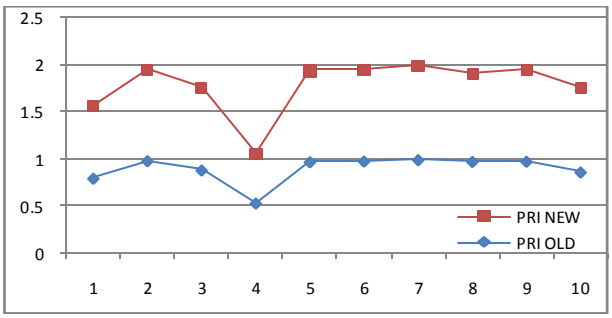


Figure (5.11) Comparative plot of PRI for Developed and Exiting Technique.

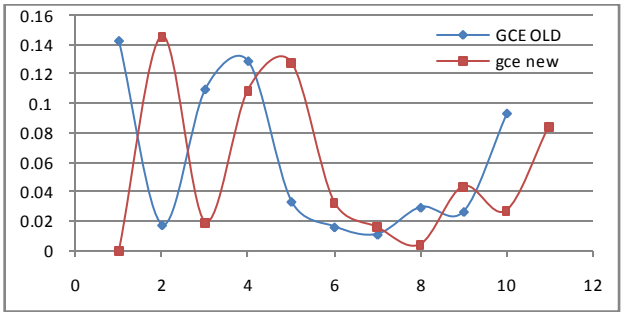


Figure (5.12) Comparative plot of VOI for Developed and Exiting Technique.

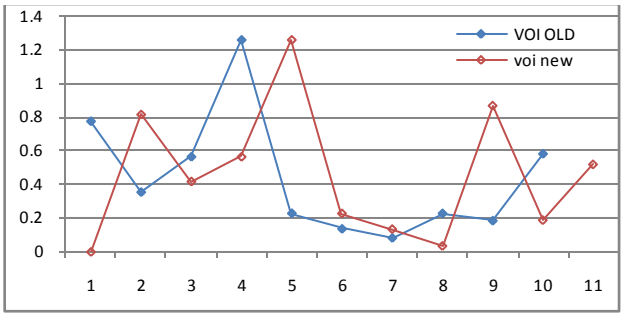


Figure (5.13) Comparative plot of GCE for Developed and Exiting Technique.

From the comparison table 1 and the comparison plots shown from figure (5.11) to figure (5.13) it is clearly observable that, the developed technique for multichannel image segmentation is much more efficient to exiting multichannel image segmentation technique. On the basis of PRI, VOI and GCE it is seen in the plots that developed technique is providing much higher PRI, smaller VOI and GCE as compare to exiting technique which leads to true segmentation capability of the developed technique over to exiting technique.

## V. CONCLUSIONS

This paper presents a level set image segmentation method based on the idea of stopping the evolving contour according to the degree of membership of the active pixel to be inside or outside of this evolving contour for the multichannel images (ie color images). It is done with the help of the FCM partition matrix. The LSE is solved by using the powerful, simple, and highly parallelizable LBM which allows the method to be a good candidate for GPU implementation. The method gives promising results. Experimental results on medical and real-world images have demonstrated the good performance of the proposed method in terms of PRI, VOI and GCE. It presents a fast and efficient comprehensive implementation for color image segmentation.

For the implementation of segmentation techniques defined for gray images, most of the time researchers determines single channel segments of the images and superimposes the single channel segment information on color images. This idea leads to provide color image segmentation using single channel segments of multi channel images. Though this method is widely adopted but doesn't provide complete true segmentation of multichannel ie color images because a color image contains three different channels for Red, green and blue components. Hence segmenting a color image, by having only single channel segments information, will definitely loose important segment regions of color images. To overcome this problem this paper deals with the development of Enhanced Level Set Segmentation for single channel Images Using Fuzzy Clustering and Lattice Boltzmann Method. For the implementation of the proposed method over color images the input color image was first divided into red, green and blue single channels then by applying the proposed single channel technique on each channels of color image will lead to three different segmentation information for red, green and blue channels. After combining all the three segmentation information true color image segments will be obtained.

The PRI, VOI, GCE value calculated for different images is found to be in a specific desired range which shows the successful implementation of the method. From the comparison table 1 and the comparison plots shown from figure (5.11) to figure (5.13) it is clearly observable that, the developed technique for multichannel image segmentation is much more efficient to exiting multichannel image segmentation technique. On the basis of PRI, VOI and GCE it is seen in the plots that developed technique is providing much higher PRI, smaller VOI and GCE as compare to exiting technique which leads to true segmentation capability of the developed technique over to exiting technique.

## REFERENCES

[1] S. Osher and J. Sethian, "Fronts propagating and curvature dependent speed: Algorithms based on Hamilton–Jacobi formulation," J. Comput.Phys., vol. 79, no. 1, pp. 12–49, Nov. 1988.

[2] M. Kass, A. Witkin, and D. Terzopoulos, "Snakes: Active contour models," Int. J. Comput. Vis., vol. 1, no. 4, pp. 321–331, Jan. 1988.

[3] V. Casselles, F. Catté, and F. Dibos, "A geometric model for active contours in image processing," Numer. Math., vol. 66, no. 1, pp. 1–31, 1993.

[4] R. Malladi, J. Sethian, and B. Vemuri, "A topology independent shape modeling scheme," in Proc. SPIE Conf. Geometric Methods Comput. Vis.II, San Diego, CA, 1993, vol. 2031, pp. 246–258.

[5] V. Caselles, R. Kimmel, and G. Sapiro, "On geodesic active contours," Int. J. Comput. Vis., vol. 22, no. 1, pp. 61–79, 1997.

[6] T. Chan and L. Vese, "Active contours without edges," IEEE Trans. Image Process., vol. 10, no. 2, pp. 266–277, Feb. 2001.

[7] W. Chen and M. L. Giger, "A fuzzy c-means (FCM) based algorithm for intensity inhomogeneity correction and segmentation of MR images," in Proc. IEEE Int. Symp. Biomed. Imaging: Nano Macro, 2004, vol. 2, pp. 1307–1310.

[8] W. M. Wells, W. E. Grimson, R. Kikinis, and F. A. Jolesz, "Adaptive segmentation of MRI data," IEEE Trans. Med.l Imag., vol. 15, no. 4, pp. 429–442, Aug. 1996.

[9] L. C. Evans and R. F. Gariepy, Measure Theory and Fine Properties of Functions. Boca Raton, FL: CRC Press, 1992.

[10] C. Li, C. Xu, C. Gui, andM. Fox, "Distance regularized level set evolution and its application to image segmentation," IEEE Trans. Image Process. vol. 19, no. 12, pp. 3243–3254, Dec. 2010.

[11] G. Aubert and P. Kornprobst, "Mathematical problems in image processing:Partial differential equations and the calculus of variations," in Applied Mathematical Sciences, vol. 147. Berlin, Germany: Springer-Verlag, 2001.

[12] Y. Chen, Z. Yan, and Y. Chu, "Cellular automata based level set method for image segmentation," in Proc. IEEE/ICME, Beijing, China, May 2007, pp. 23–27.
[13] S. Succi, The Lattice Boltzmann Equation for Fluid Dynamics and Beyond Numerical Mathematics and Scientific Computation. New York: Oxford Univ. Press, 2001.
[14] Y. Zhao, "Lattice Boltzmann based PDE solver on the GPU," Visual Comput., vol. 24, no. 5, pp. 323–333, Mar. 2007.
[15] X. He and L. Luo, "Lattice Boltzmann model for incompressible Navier–Stokes equation," J. Stat. Phys., vol. 88, no. 3/4, pp. 927–944, 1997.
[16] J. Aujol and G. Aubert, "Signed distance functions and viscosity solutions of discontinuous Hamilton–Jacobi equations," INRIA, Le Chesnay Cedex, France, 2002, inria-00072081, version 1, ref. RR-4507.
[17] J. G. Rosen, "The gradient projection method for nonlinear programming, II, nonlinear constraints," J. SIAM, vol. 9, no. 4, pp. 514–532, Dec. 1961.
[18] D. L. Pham and J. L. Prince, "Adaptive fuzzy segmentation of magnetic resonance images," IEEE Trans. Med. Imag., vol. 18, no. 9, pp. 737–752,Sep. 1999.
[19] P. L. Bhatnagar, E. P. Gross, and M. Krook, "A model for collision processes in gases. I. Small amplitude processes in charged and neutral one-component systems," Phys. Rev., vol. 94, no. 3, pp. 511–525, 1954.
[20] S. Osher and R. Fedkiw, Level Set Methods and Dynamic Implicit Surfaces. New York: Springer-Verlag, 2003.
[21] L. D. Cohen, "On active contour models and balloons," Comput. Vis. Graph., Image Process., vol. 53, no. 2, pp. 211–218, Mar. 1991.
[22] N. Paragios and R. Deriche, "Geodesic active contours for supervised texture segmentation," in Proc. IEEE Conf. CVPR, 1999, pp. I:1034–I:1040.
[23] R. Ronfard, "Region based strategies for active contour models," Int. J.Comput. Vis., vol. 13, no. 2, pp. 229–251, Oct. 1994.
[24] D. Mumford and J. Shah, "Optimal approximations by piecewise smooth functions and associated variational problems," Commun. Pure Appl .Math., vol. 42, no. 5, pp. 577–685, Jul. 1989.
[25] A. Hagan and Y. Zhao, "Parallel 3-D image segmentation of large data set on a GPU cluster," in Proc. ISVC, 2009, pp. 960–969.
[26] F. Gibou and R. Fedkiw, "A fast hybrid k-means level set algorithm for segmentation," in Proc. 4th Annu. Hawaii Int. Conf. Stat. Math., 2005,pp. 281–291.
[27] M. Bauchemin, K. Thomson, and G. Edwards, "On the Hausdorff distance used for the evaluation of segmentation results," Can. J. Remote Sens., vol. 24, no. 1, pp. 3–8, 1998.
[28] S. Chabrier, H. Laurent, C. Rosenberger, and B. Emile, "Comparative study of contour detection evaluation criteria based on dissimilarity measures,"EURASIP J. Image Video Process., vol. 2008, pp. 693 053-1–693 053-13, Feb. 2008.
[29] S. Balla-Arabé, B. Wang, and X.-B. Gao, "Level set region based image segmentation using lattice Boltzmann method," in Proc. 7th Int. Conf-Comput. Intell. Security, Sanya, China, Dec. 2011, pp. 1159–1163.
[30] D. Martin, C. Fowlkes, D. Tal, and J. Malik, "A database of human segmented natural images and its application to evaluating segmentation algorithms and measuring ecological statistics," in Proc. 8th Int. Conf . comput. Vis., Jul. 2001, vol. 2, pp. 416–423.
[31] X.-B. Gao, B.Wang, D. Tao, and X. Li, "A relay level set method for automatic image segmentation," IEEE Trans. Syst., Man, Cybern. B, Cybern.,vol. 41, no. 2, pp. 518–525, Apr. 2011.
[32] B. Wang, X.-B. Gao, D. Tao, and X. Li, "A unified tensor level set for image segmentation," IEEE Trans. Syst., Man, Cybern. B, Cybern., vol. 40, no. 3, pp. 857–867, Jun. 2010.
[33] D. R. Martin, "An empirical approach to grouping and segmentation," Ph.D. dissertation, Univ. California, Berkeley, CA, 2002.
[34] P. Sylvie and G. Laurent, "Evaluation of image segmentation: State of the art, new criteria and comparison," traitement du signal, vol. 23, no. 2, pp. 109–124, 2006.
[35] M. Polak, H. Zhang, and M. Pi, "An evaluation metric for image segmentation of multiple objects," Image Vis. Comput., vol. 27, no. 8, pp. 1223–1227, Jul. 2009.
[36] S. Balla-Arabé and X. Gao, "Image multi-thresholding by combining the lattice Boltzmann model and a localized level set algorithm," Neurocomputing, vol. 93, pp. 106–114, Sep. 2012.
[37] Z. Wang, Z. Yan, and G. Chen, "Lattice Boltzmann method of active contour for image segmentation," in Proc. 6th ICIG, 2011, pp. 338–343.
[38] J. Ding, R. Ma, J. Yang, and S. Chen, "A tree-structured framework for purifying "complex" clusters with structural roles of individual data," Pattern Recognit., vol. 43, no. 11, pp. 3753–3767, Nov. 2010.
[39] J. Ding, J. Shen, H. Pang, S. Chen, and J.-Y. Yang, "Exploiting intensity inhomogeneity to extract textured objects from natural scenes," in Proc.ACCV, 2009, vol. 3, pp. 1–10.